

12C.4

ORGANIZATION OF TROPICAL CONVECTION: DEPENDENCE OF SELF-AGGREGATION ON SST IN AN IDEALIZED MODELING STUDY

Allison A. Wing* and Kerry A. Emanuel

Program in Atmospheres, Oceans, and Climate, Massachusetts Institute of Technology, Cambridge, MA

1. INTRODUCTION

Convective cloud clusters are responsible for most of the rainfall and cloudiness over the tropics, with approximately 50% of rainfall in the tropics due to mesoscale convective systems (Nesbitt et al., 2000). This allows tropical cloud clusters to modulate the radiative heating and cooling rates of the surface and atmosphere and influence the large-scale circulation and moisture distribution. In idealized modeling studies, the development of large-scale convective organization through self-aggregation alters the mean temperature and moisture profiles and radiative fluxes, highlighting the effect of organized convection on variables important to climate. The phase change into an aggregated state is accompanied by a dramatic drying of the entire domain. A systematic dependence of water vapor, turbulent surface fluxes, and radiation on the degree of convective aggregation is also found in observations (Tobin et al., 2011). They found that when deep convection is more aggregated, there is a decrease in the free tropospheric humidity in the convection-free environment, enhanced turbulent surface fluxes within and outside convective areas, and reduced low-mid level cloudiness in the environment. Therefore, understanding how and why tropical convection organizes is important for understanding both tropical and global climate variability, and climate sensitivity. In this study, the problem is approached through the context of idealized modeling of convective organization in radiative - convective equilibrium using a cloud - resolving model. Previous studies have investigated interactions between the environment and the convection that allow convection to self-aggregate into a single cluster, and have found this self-aggregation to be dependent on a sea surface temperature threshold (Khairoutdinov and Emanuel, 2010). To examine the nature of this threshold, the System for Atmospheric Modeling is used to perform 3-d cloud resolving simulations at different sea surface temperatures. Simulations in which aggregation does occur are then closely com-

pared to those in which it does not, via analysis with a moisture sorted streamfunction. Sensitivity experiments are then performed to determine the relevant feedback mechanism that controls the SST dependence of self-aggregation. This study investigates three basic questions:

- How does self-aggregation evolve?
- What physical mechanisms are important?
- How and why does self-aggregation depend on sea surface temperature?

2. MODEL SIMULATIONS

The model used is the System for Atmospheric Modeling, henceforth referred to as SAM (Khairoutdinov and Randall, 2003). SAM is a three-dimensional cloud resolving model that solves the anelastic equations of motion. The prognostic thermodynamics variables are the total nonprecipitating water, total precipitating water, and the liquid water/ice static energy, h_L

$$h_L = c_p T + gz - L_c(q_c + q_r) - L_s(q_i + q_s + q_g) \quad (1)$$

where q_c is cloud water mixing ratio, q_r is rain mixing ratio, q_i is cloud ice mixing ratio, q_s is snow mixing ratio, q_g is graupel mixing ratio, L_c is the latent heat of evaporation, and L_s is the latent heat of sublimation. The simulations discussed here were performed with a domain size of $768 \times 768 \text{ km}^2$ with 64 vertical levels and rigid lid at 28 km. The horizontal resolution was 3 km, and a doubly periodic lateral boundary condition was employed. The model was initialized with a sounding from the domain average of a smaller domain run in radiative-convective equilibrium and white noise in the boundary layer temperature field. There is no mean wind or other external forcing imposed. We used a fully interactive RRTM radiation scheme, with solar insolation constant and equal to a value of 413.98 W/m^2 and no diurnal cycle. The surface sensible and latent heat

*Corresponding author address: Allison A. Wing, Massachusetts Institute of Technology 54-1815, Cambridge, MA 02139; email: awing@mit.edu

fluxes were computed interactively. Finally, we performed simulations at fixed sea surface temperature (SST), with values between 298K and 312K.

3. REVIEW OF SELF-AGGREGATION

Tropical convection is often viewed as a quasi-equilibrium process in which convective clouds consume convective available potential energy at the same rate it is supplied by large-scale processes (Emanuel et al., 1994). The simplest form of such an equilibrium is radiative-convective equilibrium, in which convection is balanced by radiative cooling and heat transfer from the surface. On large enough space and time scales, the tropics can be thought of as in radiative-convective equilibrium, although it is never actually observed at a given time/place due to the presence of large-scale circulations in the atmosphere. Nevertheless, radiative-convective equilibrium is a good starting point for understanding tropical dynamics. Simulations of convection in radiative-convective equilibrium using three-dimensional cloud system resolving models often produce distributions of convection that are nearly random in space and in time. Figure 1 shows an example of this with a snapshot of the outgoing longwave radiation, indicating the existence of high clouds from one of the simulations.

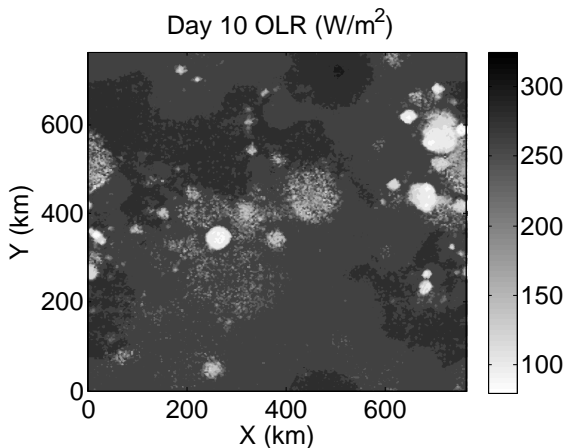


Figure 1: Snapshot of outgoing longwave radiation at day 10 of radiative-convective equilibrium simulation.

However, when certain conditions are met, the convection becomes organized into a single, intensely convecting moist clump surrounded by a broad region of dry subsiding air (Bretherton et al., 2005; Nolan et al., 2007). Figure 2 is a snapshot of the outgoing longwave radiation from a later time in the same simulation as Figure 1, showing how all the clouds are confined to a single cluster. Convection is often thought of as being organized by external influ-

ences such as large-scale sea surface temperature (SST) gradients or wind shears.

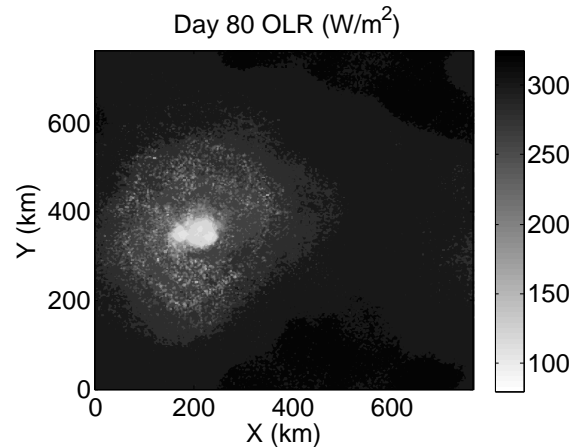


Figure 2: Snapshot of outgoing longwave radiation at day 80 of a radiative-convective equilibrium simulation.

However, in this case, the convection is self-organizing through interactions between the environment and the convection and radiation - termed "self-aggregation".

Previous work indicated that cloud-water vapor-radiation feedbacks that dry the drier air columns and moisten the moister air columns are essential to the self-aggregation process (Tompkins, 2001; Bretherton et al., 2005; Muller and Held, 2012). Deep convection can more easily develop where the middle-troposphere is already moist and then tends to keep the middle and upper troposphere moist where it is convecting. Surface flux feedbacks may also play a role (Bretherton et al., 2005), with the moistest columns having slightly enhanced heat fluxes in the early stages of self-aggregation because of convective gustiness. Khairoutdinov and Emanuel (2010) found that self-aggregation only occurred above an SST threshold. A key objective of this project is to determine the exact nature of this threshold and how it can be overcome. There are also indications that self-aggregation is sensitive to the dimensionality, domain size, and horizontal resolution of the simulations, with it being favored by large domains and relatively coarse resolution (Stephens et al., 2008; Muller and Held, 2012).

4. METHODS

To compare a case in which self-aggregation did occur with one in which it did not, we will employ a moisture-sorted streamfunction, following the work of Bretherton et al. (2005). We take a daily average, and then horizontally average over $48 \times 48 \text{ km}^2$

blocks to focus on the mesoscale organization. An example of a daily and block averaged field is shown in Figure 3, where the cloud cluster is easily identifiable as the region of high column relative humidity. Here, column relative humidity (CRH) is defined as the total precipitable water (TPW) divided by the saturated water vapor path (SWP).

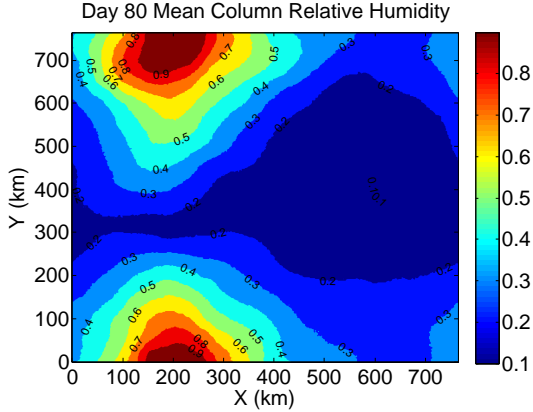


Figure 3: Block averaged day 80 mean column relative humidity for simulation at 305 K.

We then sort the blocks according to their column relative humidity. Once we have this sorting function, we can apply it to other fields, such as the daily averaged vertical velocity. We then calculate a streamfunction using the CRH-sorted vertical velocity by integrating from the dry to moist columns.

$$\psi_i(z) = \psi_{i-1}(z) + \sum_i \rho(z) w_{i-1}(z) \quad (2)$$

The streamfunction represents the vertical mass flux accumulated over the i driest columns. Negative values represent circulations in a counterclockwise sense, positive values represent circulations in a clockwise sense. In addition, we sort the block-averaged frozen moist static energy and cloud condensates by column relative humidity, and display those fields, along with the streamfunction, as a function of height and moisture space (each block is ranked by its CRH, with the lowest ranks being the driest blocks). The frozen moist static energy is given by

$$FMSE = c_p T + gz + L_c q_v - L_f q_{ice} \quad (3)$$

where L_f is the latent heat of fusion and q_{ice} represents all ice phase condensates.

5. RESULTS

Figure 4 summarizes the results of simulations at different values of SST. An obvious feature is a dramatic increase in the domain averaged outgo-

ing longwave radiation after self-aggregation occurs, allowing this to be used as a metric for whether or not self-aggregation occurred. The simulations at SST's of 301K, 303K, 305K and 307K self-aggregated, while the runs at colder and higher values of SST did not. Based on previous work, we expected that self-aggregation would not occur at the coldest SST's, but it was a bit more surprising that it did not occur at the highest SST's (310K and 312K). A possible explanation for this behavior is that a larger domain size is needed for a cluster to form at those warmer temperatures. The hypothesis is that the stratification is larger at higher SST's, so the subsidence surrounding the cluster is weaker and would therefore need to cover a larger area. With a fixed domain size of $768 \times 768 \text{ km}^2$ in the horizontal, there may not be enough space for that to occur in the simulations at 310K and 312K. This hypothesis will be tested in future work. Also note in Figure 4 that the time to aggregation does not vary monotonically with SST, indicating a possibly large stochastic component to self-aggregation.

Figure 10 and Figure 11 compare the evolution of the cluster for the run at 298K, which did not self-aggregate, to the run at 305K, which did self-aggregate. Figure 10 shows plan views of daily mean total precipitable water. Figure 11 shows the moisture-sorted streamfunction described in the previous section and the frozen moist static energy in height and moisture space. Again, these plots should be interpreted as going from dry areas (on the left) to moist areas (on the right), and all fields are daily averages. First, we examine the right column of Figure 10, which shows the TPW for the 305K run. At day 10, the TPW field is mostly homogeneous, with a small patch a bit drier than the rest. By day 50, that small dry patch has expanded to be much larger, and by day 80, it has forced all the moisture into a single cluster, where the highest values of TPW are concentrated. Outside that moist cluster, the rest of the domain has very low values of TPW. Turning to the right column of Figure 11, we see that at day 10 (top right image), the frozen moist static energy is fairly homogeneous and there are clouds throughout the domain. There is a counterclockwise circulation, indicated by the streamfunction, in the mid to upper troposphere. By day 50, the circulation has strengthened and extended to the surface, with a secondary circulation in the low levels. In concert with this, the gradient of frozen moist static energy between the dry and moist regions has strengthened, including at the lowest levels. This enables the low level circulation to transport frozen moist static energy up gradient from the dry to moist regions (consistent with

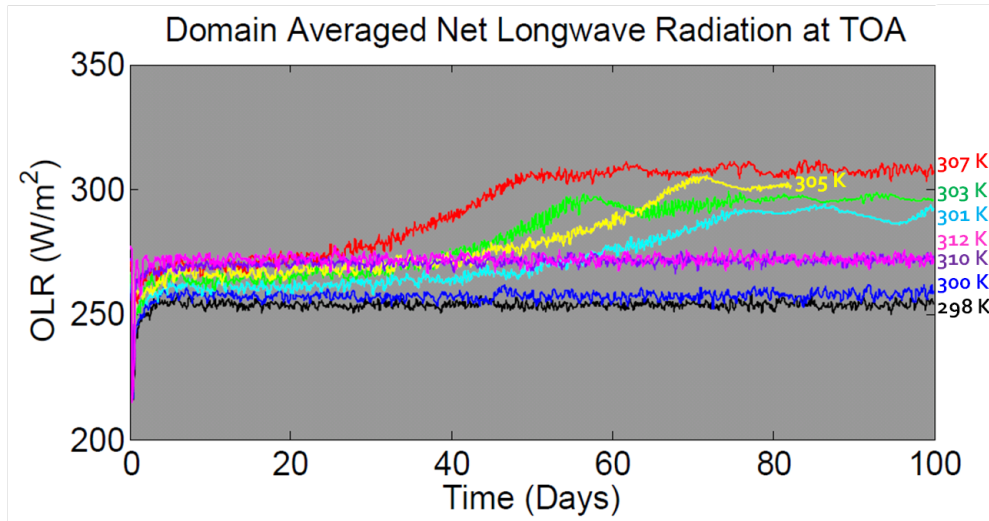


Figure 4: Evolution of the domain averaged outgoing longwave radiation. Each curve is a simulation performed at a different fixed SST. The data are hourly averages.

previous studies). At day 80, the cluster is mature with the ascent and clouds confined to the moistest regions and a strong gradient in frozen moist static energy between the moist and dry regions.

We now compare to the evolution of a case that did not self-aggregate, the 298K run. Focusing on the left column of Figure 10, we see that the daily mean total precipitable water is approximately homogenous at each time shown, with no dry patches forming or expanding as we saw in the 305K case. At day 10, the image in Figure 11 looks qualitatively similar to the 305K case. There is a circulation in the middle-upper troposphere and no gradient in frozen moist static energy. The difference is that as we move to days 50 and 80, the circulation never is able to establish it self as it did in the 305K case. It never extends all the way to the surface, and there is no development of a frozen moist static energy gradient that enables the circulation to self-amplify.

Now that we have examined how the evolution of the simulation differs at different SST's, we examine how the strength of the cluster depends on the SST of the simulation. Figure 5 shows the evolution of the strength of the cluster, for the four runs that did self-aggregate, with time. Here we define the strength of the cluster as the difference between the 95th and 25th percentiles of column relative humidity. Two things are notable from this figure. First, there is a huge increase in the column relative humidity difference as aggregation occurs. In the aggregated state, there is a much larger gap in the column relative humidity of the moister and dryer areas. Second, the CRH difference in the aggregated state is roughly in-

dependent of temperature, with all four runs roughly converging.

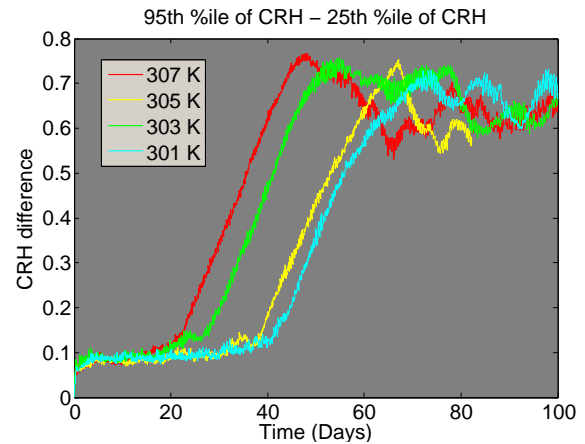


Figure 5: Evolution of the strength of the cloud cluster for the runs that did self-aggregate.

This is not the case if we were to use an absolute metric of cluster strength, such as the difference between the 95th and 25th percentiles of total precipitable water. In that case (not shown), the strength of the cluster appears to be stronger at higher SSTs, mostly due to the exponential increase of water vapor with temperature following the Clausius-Clapeyron relation. The 95th percentile of TPW increases much more with higher SST than the 25th percentile does. However, when we normalize by the saturated water vapor path and use column relative humidity as our metric, this normalized strength metric does not vary much with temperature, as shown by Figure 5.

Regarding possible mechanisms controlling the de-

pendence of self-aggregation on SST, two contenders based on previous studies are the moisture-convection and cloud-radiation feedbacks. Figure 6 shows the anomaly of the day 80 mean water vapor mixing ratio from the initial conditions for the 305K run, which did self-aggregate. We see a massive drying of the dry regions and moistening of the moist regions. The largest anomalies are in the lower troposphere, although the very moistest columns are quite a bit moister throughout a substantial portion of the column. These are huge anomalies, with the dry regions losing nearly all their water vapor (anomalies of -15 g/kg!). Since moist regions favor future convection, and convection causes moistening, the moisture-convection feedback is a positive feedback that favors self-aggregation. If this feedback were for some reason stronger at higher SSTs, that could explain the observed dependence of self-aggregation on SST.

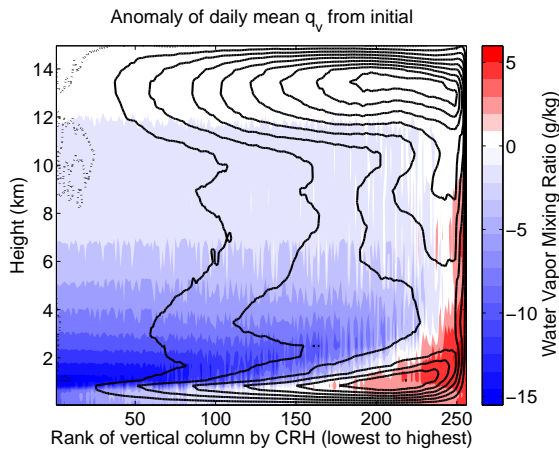


Figure 6: Shading is anomaly of day 80 mean water vapor mixing ratio from initial condition, for 305K run. Contours are moisture-sorted streamfunction.

Figure 7 addresses the radiative feedback mechanism, by showing the vertically averaged radiative heating rate at day 80 for the 305K run. The vertically averaged radiative heating rate is nearly zero in the moistest columns where the clouds are concentrated. In the dry regions, there is strong radiative cooling. If this enhanced cooling of the driest columns and warming of the moistest columns was stronger at higher SST, this could also play a role in explaining the dependence of self-aggregation on SST.

A third possible mechanism is surface flux feedbacks. We find that a smaller gust factor in the surface flux calculation favors self aggregation. As an example, we consider the 301K run. With a gust factor of 1 m/s, the model self-aggregates and a cluster forms, as indicated by the blue line in Figure 8 and

the left panel of Figure 9. However, when the gust factor is increased to 4 m/s, which is represented by the cyan line in Figure 8, self-aggregation does not occur.

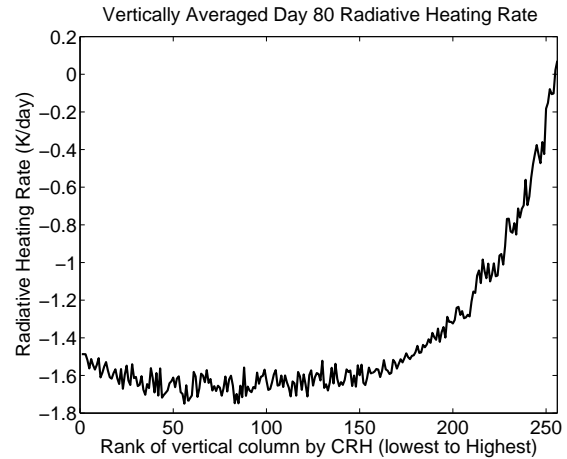


Figure 7: Vertically averaged day 80 mean radiative heating rate, for 305K run.

We note that increasing the gust factor does not completely prevent self-aggregation, as the right panel of Figure 9 does indicate a dry patch forming, but causes it to proceed much slower. If run for longer than 100 days, perhaps that simulation would eventually self-aggregate. The mechanism at play is two-fold. With a lower gust factor, one needs a larger air-sea enthalpy disequilibrium to get a strong surface flux, making surface flux feedbacks more likely. Second, with a lower gust factor, it takes less real gustiness to differentiate between convecting and non-convecting regions. The gusts are thus more effective at amplifying the surface fluxes in the convective regions.

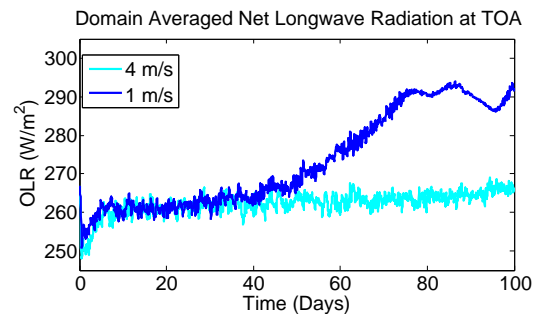


Figure 8: Evolution of domain averaged outgoing longwave radiation at an SST of 301K, for a simulation with a 4 m/s gust factor (cyan) and a simulation with a 1 m/s gust factor (blue).

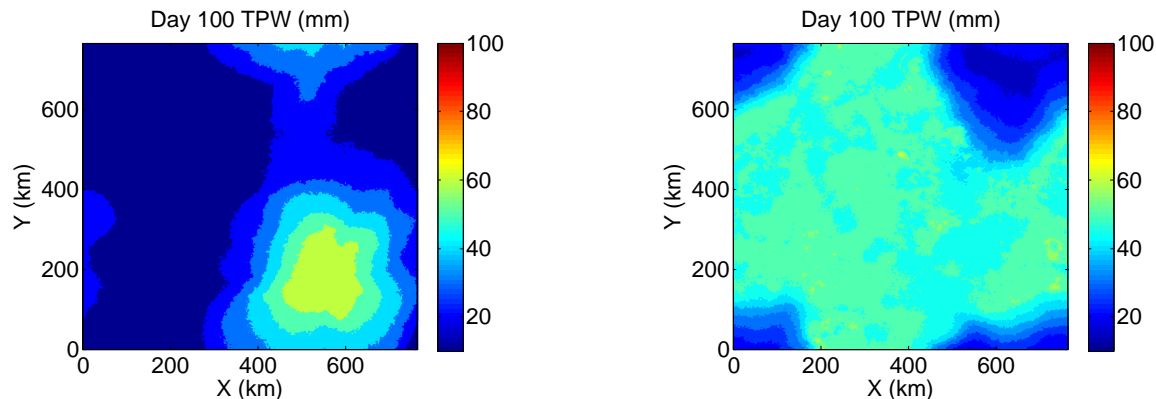


Figure 9: Day 100 total precipitable at SST of 301K. Left panel: gust factor of 1 m/s. Right panel: gust factor of 4 m/s.

6. FUTURE WORK

The results discussed here are preliminary, and more work needs to be done to address the questions indicated in the introduction section. In particular, we are continuing work to determine which of the potential feedback mechanisms are temperature dependent and how those dependencies explain why self-aggregation is less favored at low SST. In addition, to further characterize the nature of the SST threshold, we will investigate what is needed to force the system to aggregate when it is below that threshold. We will also investigate to what degree (if any) self-aggregation is a stochastic process. Finally, we will explore the robustness of self-aggregation to alternate model setups, such as a weak temperature gradient set up (instead of radiative-convective equilibrium).

7. ACKNOWLEDGEMENTS

We would like to acknowledge high-performance computing support provided by NCAR's Computational and Information Systems Laboratory, sponsored by the National Science Foundation. Funding support for Allison A. Wing is from the MIT Joint Program on the Science and Policy of Global Change.

8. REFERENCES

- Bretherton, C., P. Blossey, and M. Khairoutdinov, 2005: An energy-balance analysis of deep convective self-aggregation above uniform SST. *J. Atmos. Sci.*, **62**, 4237–4292.
- Emanuel, K., J. Neelin, and C. Bretherton, 1994: On large-scale circulations in convecting atmospheres. *Quart. J. Roy. Meteor. Soc.*, **120**, 1111–1143.
- Khairoutdinov, M. and D. Randall, 2003: Cloud resolving modeling of the ARM summer 1997 IOP: Model formulation, results, uncertainties, and sensitivities. *J. Atmos. Sci.*, **60**, 607–625.
- Khairoutdinov, M. F. and K. Emanuel, 2010: Aggregation of convection and the regulation of tropical climate. Preprints. *29th Conference on Hurricanes and Tropical Meteorology*, Tucson, AZ, Amer. Meteorol. Soc.
- Muller, C. and I. Held, 2012: Detailed investigation of the self-aggregation of convection in cloud resolving simulations. *J. Atmos. Sci.*, accepted.
- Nesbitt, S., E. Zipser, and D. Cecil, 2000: A census of precipitation features in the tropics using TRMM: Radar, ice scattering, and lightning observations. *J. Climate*, **13**, 4087–4106.
- Nolan, D., E. Rappin, and K. Emanuel, 2007: Tropical cyclonegenesis sensitivity to environmental parameters in radiative-convective equilibrium. *Q. J. R. Meteorol. Soc.*, **133**, 2085–2107.
- Stephens, G., S. van den Heever, and L. Pakula, 2008: Radiative-convective feedbacks in idealized states of radiative-convective equilibrium. *J. Atmos. Sci.*, **65**, 3899–3916.
- Tobin, I., S. Bony, and R. Roca, 2011: Observational evidence for a systematic dependence of water vapor, surface fluxes, and radiation on the degree of aggregation of deep convection. *J. Atmos. Sci.*, submitted.
- Tompkins, A., 2001: Organization of tropical convection in low wind shears: the role of water vapor. *J. Atmos. Sci.*, **58**, 529–545.

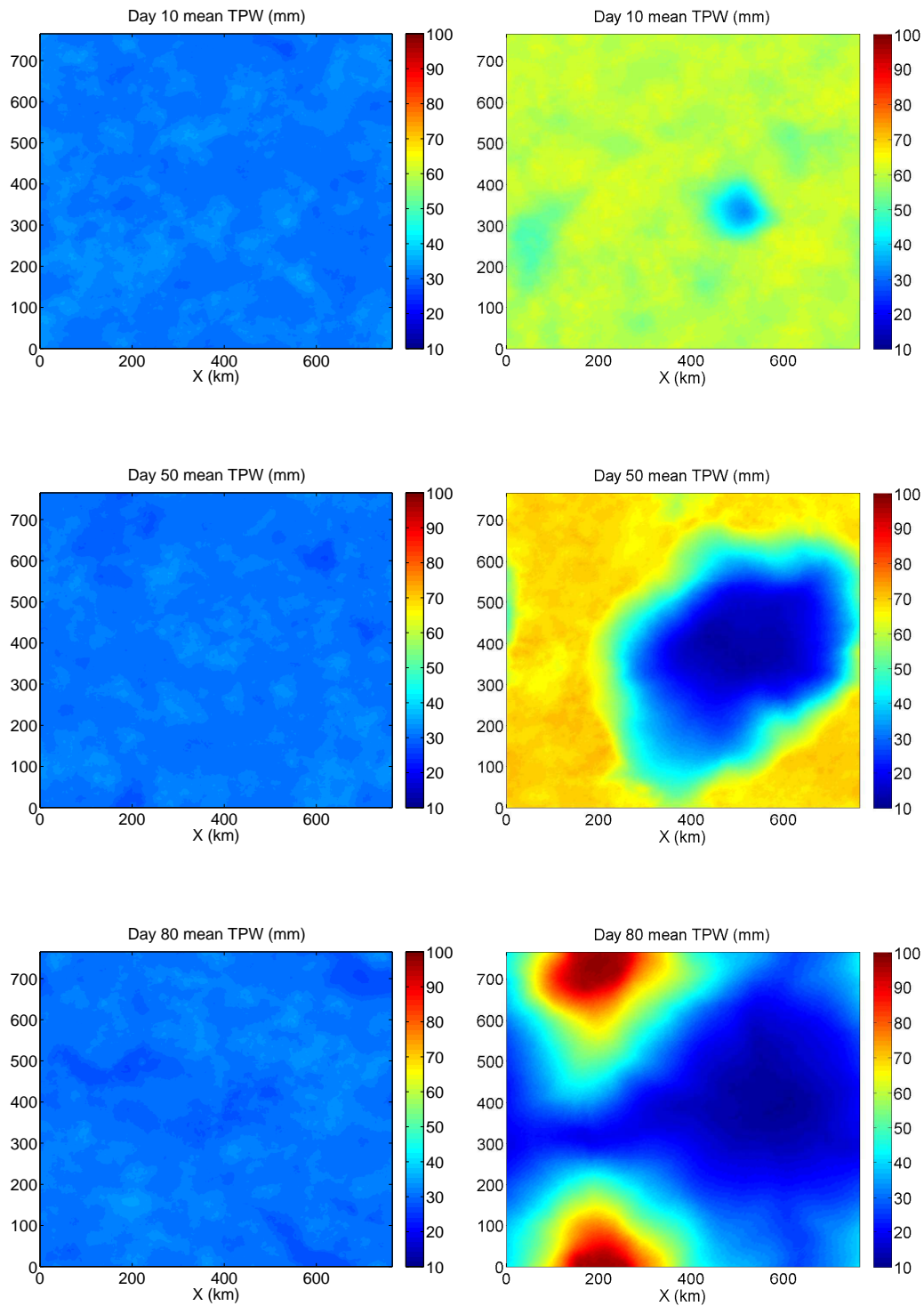


Figure 10: Left column: evolution of self-aggregation for case at 298K. Right column: evolution of self-aggregation for case at 305K. Top row: Day 10. Middle row: Day 50. Bottom row: Day 80. Plotted is the daily averaged total precipitable water.

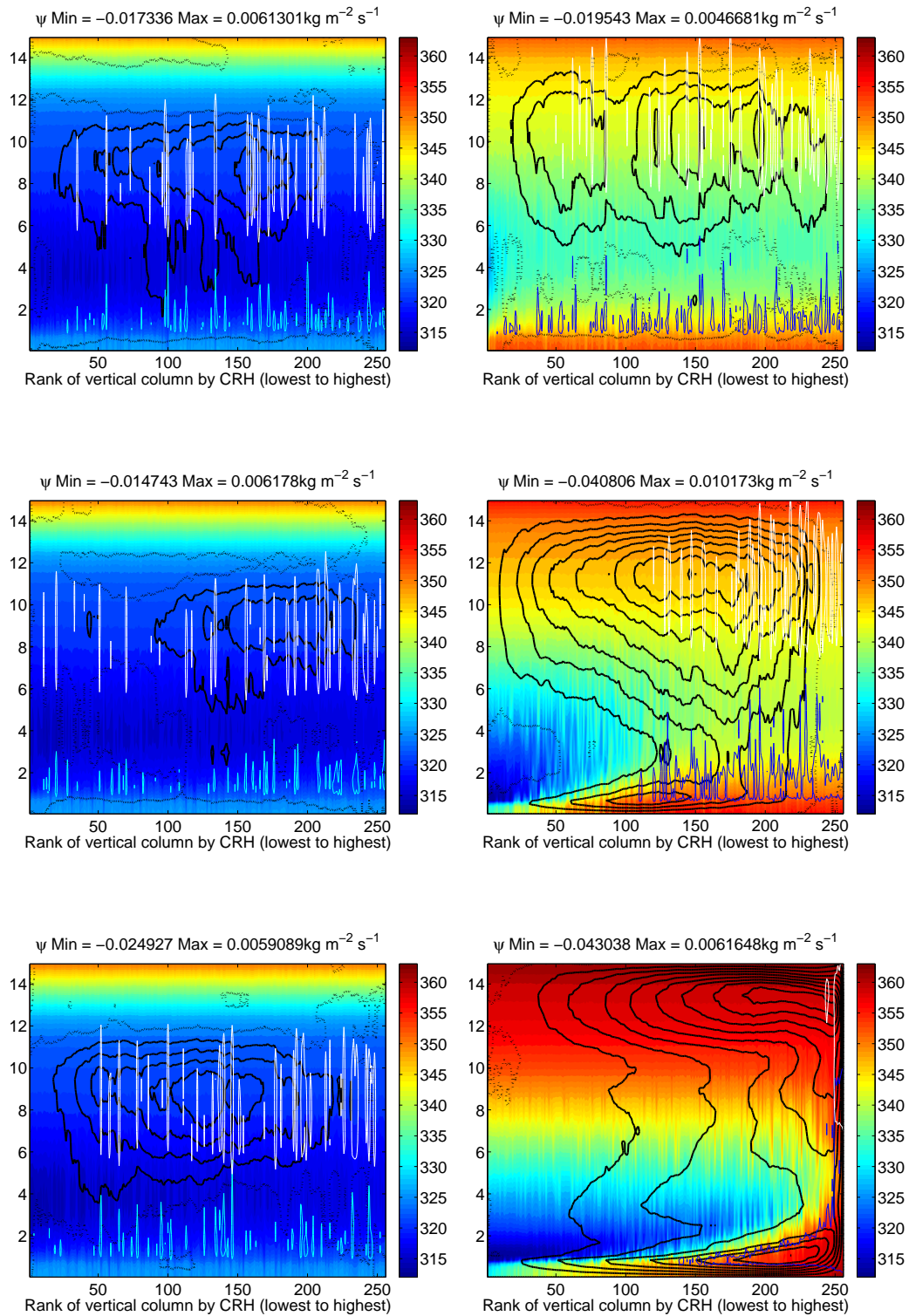


Figure 11: Left column: evolution of self-aggregation for case at 298K. Right column: evolution of self-aggregation for case at 305K. Top row: Day 10. Middle row: Day 50. Bottom row: Day 80. Plotted is the frozen moist static energy ($kJkg^{-1}$, shading), negative values of the streamfunction ($kgm^{-2}s^{-1}$, solid black contours), positive values of the streamfunction ($kgm^{-2}s^{-1}$, dotted black contours), 0.01 g/kg ice cloud condensate contour (white contours), and 0.01 g/kg liquid cloud condensate contour (blue contours). All are daily and block-averaged. On the x-axis, dry regions are on the left and moist regions are on the right.